HHS Public Access

Author manuscript

Sci Transl Med. Author manuscript; available in PMC 2018 August 16.

Published in final edited form as:

Sci Transl Med. 2017 August 16; 9(403): . doi:10.1126/scitranslmed.aai7459.

$mGlu_7$ potentiation rescues cognitive, social, and respiratory phenotypes in a mouse model of Rett syndrome

Rocco G. Gogliotti[1,2], **Rebecca K. Senter**[1,2], **Nicole M. Fisher**[1,2], **Jeffrey Adams**[1,2], **Rocio Zamorano**[1,2], **Adam G. Walker**[1,2], **Anna L. Blobaum**[1,2], **Darren W. Engers**[1,2], **Corey R. Hopkins**[1,2,3], **J. Scott Daniels**[1,2], **Carrie K. Jones**[1,2], **Craig W. Lindsley**[1,2,3], **Zixiu Xiang**[1,2], **P. Jeffrey Conn**[1,2,4], and **Colleen M. Niswender**[1,2,4,*]

[1]Department of Pharmacology, Vanderbilt University, Nashville, TN 37232, USA

[2]Vanderbilt Center for Neuroscience Drug Discovery, Vanderbilt University, Nashville, TN 37232, USA

[3]Department of Chemistry, Vanderbilt University, Nashville, TN 37232, USA

[4]Vanderbilt Kennedy Center, Vanderbilt University Medical Center, Nashville, TN 37232, USA

Abstract

Rett syndrome (RTT) is a neurodevelopmental disorder caused by mutations in the *methyl-CpG binding protein 2* (*MECP2*) gene. The cognitive impairments seen in mouse models of RTT correlate with deficits in long-term potentiation (LTP) at Schaffer collateral (SC)–CA1 synapses in the hippocampus. Metabotropic glutamate receptor 7 ($mGlu_7$) is the predominant mGlu receptor expressed presynaptically at SC-CA1 synapses in adult mice, and its activation on GABAergic interneurons is necessary for induction of LTP. We demonstrate that pathogenic mutations in *MECP2* reduce $mGlu_7$ protein expression in brain tissue from RTT patients and in MECP2-deficient mouse models. In rodents, this reduction impairs $mGlu_7$-mediated control of synaptic transmission. We show that positive allosteric modulation of $mGlu_7$ activity restores LTP and improves contextual fear learning, novel object recognition, and social memory. Furthermore, $mGlu_7$ positive allosteric modulation decreases apneas in *Mecp2*$^{+/-}$ mice, suggesting that $mGlu_7$ may be a potential therapeutic target for multiple aspects of the RTT phenotype.

*Corresponding author. colleen.niswender@vanderbilt.edu.

SUPPLEMENTARY MATERIALS

www.sciencetranslationalmedicine.org/cgi/content/full/9/403/eaai7459/DC1

Materials and Methods

Author contributions: R.G.G., R.K.S., N.M.F., A.G.W., and C.M.N. designed, performed, and analyzed the molecular, phenotypic, and electrophysiology experiments. R.Z. and C.M.N. performed and analyzed the in vitro pharmacology assays, and J.A. and R.G.G. performed the WBP assays. A.L.B. and J.S.D. conducted the LC MS/MS, plasma binding, and protein binding experiments for DMPK analysis, and D.W.E. and C.R.H. synthesized the compounds used herein. C.K.J. assisted in the design of behavioral assays, C.W.L. oversaw chemical optimization, Z.X., P.J.C., and C.M.N. supervised electrophysiology experiments, and P.J.C. and C.M.N. oversaw molecular pharmacology experiments. R.G.G., R.K.S., and C.M.N. wrote and edited the paper with input from all authors.

Competing interests: The authors declare that they have no competing interests.

Data and materials availability: The data for each graph have been presented in the figure legends and in the body of the text.

INTRODUCTION

Rett syndrome (RTT) is an X-linked neurodevelopmental disorder that is caused by loss-of-function mutations in the *methyl-CpG binding protein 2* (*MECP2*) gene (1). Patients with RTT develop relatively normally for the first 6 to 18 months of life, after which they undergo severe developmental regression coinciding with the presentation of seizures, cognitive impairments, apneas, and the loss of language and motor skills (2). Although MECP2 is ubiquitously expressed, almost all symptoms of RTT can be recapitulated when the protein is removed exclusively from the central nervous system in mice (3). Cell-specific knockout and rescue experiments in mice have linked MECP2 deficiency in neuronal subpopulations to distinct aspects of the RTT phenotype, with the most marked effects observed when MECP2 is depleted in GABAergic neurons (4–8). Among other proposed functions, MECP2 can act to either repress or activate transcription of genes in the brain (9). Hence, several large-scale microarray studies have been performed to identify genes specifically regulated by MECP2 (10, 11). These studies, however, have failed to find gross changes in gene expression and have identified few targets regulated by MECP2 that are amenable to drug development (12, 13).

Metabotropic glutamate receptor 7 ($mGlu_7$) is a heterotrimeric GTP-binding protein–coupled receptor (GPCR) highly expressed in brain regions affected in RTT (14, 15), such as the cortex, hippocampus, striatum, and brainstem (16). $mGlu_7$ is the protein product of the *GRM7* gene, which is epigenetically regulated by the methylation status of its promoter (17). $mGlu_7$ is expressed presynaptically at both GABAergic and glutamatergic synapses and acts to decrease neurotransmitter release when stimulated (18, 19). Mouse models of RTT display attenuated long-term potentiation (LTP) at Schaffer collateral (SC)–CA1 synapses in the hippocampus, as well as deficits in hippocampal-based learning and memory tasks consistent with the cognitive impairments present in RTT patients (20–22). Because we have previously demonstrated that $mGlu_7$ is necessary for induction of LTP at SC-CA1 (23), we hypothesized that the electrophysiological changes and behavioral deficits observed in RTT model mice could be, in part, due to impaired $mGlu_7$ signaling. This hypothesis is further supported by the fact that $mGlu_7$ knockout mice also display deficits in hippocampal readouts of learning and memory, similarly to RTT animals (24, 25).

Here, we demonstrate that the expression of $mGlu_7$, a GPCR highly amenable to drug development (26), is decreased in the motor cortex of human RTT autopsy samples and in both *Mecp2*$^{-/y}$ and *Mecp2*$^{+/-}$ mouse models of RTT. We also show that reduced $mGlu_7$ expression in the hippocampus produces a functional deficit in $mGlu_7$-modulated control of synaptic transmission at SC-CA1 synapses, which can be restored by application of two structurally distinct $mGlu_7$ positive allosteric modulators (PAMs), VU0422288 and VU0155094 (26). Finally, we establish that VU0422288 pretreatment can reverse deficits in contextual fear memory, social recognition, and apneas in RTT model mice. Together, these results suggest that potentiation of $mGlu_7$ may serve as a viable therapeutic approach to treating cognitive and respiratory impairments in RTT.

RESULTS

MECP2 activates *GRM7* transcription in vitro

MECP2 was initially identified as a transcriptional repressor; however, it can also activate gene transcription (9). To determine whether MECP2 acts as a transcriptional activator or repressor at the *GRM7* locus, we generated a reporter construct containing either 1000 base pairs of the human *GRM7* promoter or the minimal pGL4 promoter alone upstream of a luciferase gene (Fig. 1A). Both the minimal promoter and the *GRM7*-containing constructs were then transfected into human embryonic kidney (HEK) 293 cells with or without human *MECP2*, and the expression of luciferase was measured by calculating the relative luciferase units (RLU) compared to transfection of a *Renilla* control vector. We observed no significant change in luciferase expression with the minimal promoter construct with or without *MECP2* (Fig. 1B). Conversely, a significant increase in RLU was observed relative to pGL4 alone when the pGL4/*GRM7* construct was transfected with either 37.5 or 75.0 ng of *MECP2* ($P < 0.0001$; Fig. 1B), suggesting that MECP2 is an activator at this locus in vitro.

$mGlu_7$ expression is reduced in human motor cortical tissue

To determine whether our in vitro characterization of MECP2-*GRM7* dynamics translated in vivo, we acquired primary motor cortex samples [Brodmann area 4 (BA4)] from seven female patients diagnosed with *MECP2* mutation–positive RTT and eight unaffected female control samples matched for age and postmortem interval (table S1). From these samples, we measured *GRM7* expression using quantitative real-time polymerase chain reaction (qRT-PCR) and $mGlu_7$ expression using Western blot analysis. We also probed BA4 Western blots for vesicular glutamate transporter 2 (vGlut2) to assess for potential RTT-specific tissue degradation and/or nonspecific increases or decreases in presynaptic proteins. In these experiments, we observed no significant reduction in *GRM7* mRNA expression ($P = 0.07$), a significant decrease in $mGlu_7$ protein ($P < 0.001$), and no change in vGlut2 expression (Fig. 1, C to F). We previously reported a decrease in MECP2 expression in this sample set (12). These data are in agreement with the hypothesis that MECP2 is an activator of $mGlu_7$ expression and that this relationship is conserved in brain samples from RTT patient autopsy samples.

$mGlu_7$ mRNA and protein expression is reduced in *Mecp2*$^{-/y}$ mice

We next performed studies to determine whether loss of *Mecp2* also results in decreased *Grm7* expression in a mouse model of RTT [B6.129P2(C)-*Mecp2*$^{tm1.1Bird}$/J; *Mecp2*$^{-/y}$], relative to an *Mecp2*$^{+/y}$ control group, to assess the contribution of decreased $mGlu_7$ to the RTT phenotype (27). In contrast to human motor cortex samples, we detected significantly reduced *Grm7* mRNA expression in the total cortex ($P < 0.05$) and striatum ($P < 0.001$) of symptomatic *Mecp2*$^{-/y}$ mice with qRT-PCR {"symptomatic" was defined as the presence of hindlimb clasping and body tremor [postnatal day 39 (P39) to P55]} (Fig. 2A).

To determine whether $mGlu_7$ protein expression was also decreased, we performed Western blotting on total protein preparations and detected significant reductions in total $mGlu_7$ expression in the cortex ($P < 0.05$) but not in the hippocampus or striatum (Fig. 2, B and C). The specificity of our $mGlu_7$ antibody was validated using brain tissue from $mGlu_7$

knockout mice (fig. S1). Because functional $mGlu_7$ is expressed presynaptically within the synaptic cleft (16, 18, 19), we also prepared synaptosomes from the cortex and hippocampus to isolate synaptic $mGlu_7$. We observed a significant $mGlu_7$ decrease in hippocampal ($P < 0.001$), but not cortical, synaptosomes (Fig. 2, D and E), suggesting that the amount of synaptic $mGlu_7$ does not correlate with total cellular $mGlu_7$ in all contexts. To confirm that reductions in *Grm7* and $mGlu_7$ were consistent with the loss of *Mecp2*, we profiled the expression patterns of the known MECP2 target gene *glutamate decarboxylase 2* (*Gad2*; encoding Gad65) (4) as well as of a gene previously shown to be unaffected by *Mecp2* mutations, *metabotropic glutamate receptor 4* (*Grm4*; encoding $mGlu_4$). We detected a significant decrease in *Gad2* expression but no change in *Grm4* expression (fig. S2, A and B) (28). Furthermore, we probed cortical and hippocampal synaptosome blots for vGlut2 and found no change in expression, thereby suggesting that a nonspecific decrease in presynaptic structures is likely not the cause of $mGlu_7$ reduction (Fig. 2D and fig. S2C). Together, these results support the hypothesis that the loss of MECP2 results in a reduction in $mGlu_7$ expression in total cortex and in hippocampal synaptic structures.

Loss of Mecp2 impairs $mGlu_7$ function at SC-CA1 synapses

Application of $mGlu_7$ agonists is known to decrease field excitatory post-synaptic potentials (fEPSPs) at SC-CA1 synapses in rodents (23, 26, 29). To determine whether decreased hippocampal $mGlu_7$ synaptic protein expression correlated with disrupted $mGlu_7$-mediated synaptic transmission, we examined the effects of the agonist LSP4-2022 (30). LSP4-2022 activates $mGlu_4$, $mGlu_7$, and $mGlu_8$; however, we attribute the effects of LSP4-2022 at SC-CA1 synapses to $mGlu_7$ activation because (i) $mGlu_7$ is the only presynaptic mGlu receptor at SC-CA1 synapses in adult mice (26, 31) and (ii) the effects of LSP4-2022 on SC-CA1 synaptic transmission are completely blocked by an $mGlu_7$-selective negative allosteric modulator (NAM), ADX71743 (23, 29). Similar to previous studies (20, 21), we observed altered basal synaptic properties in hippocampal slices from symptomatic $Mecp2^{-/y}$ mice in response to paired-pulse stimulation [0.05 Hz, 20-ms interstimulus interval (ISI)], including an enhanced input-output curve and a reduction in paired-pulse ratio (PPR) (fig. S3). To determine whether there were differences in $mGlu_7$ function in $Mecp2^{-/y}$ mice, we recorded fEPSPs after a 10-min bath application of 30 μM LSP4-2022. In $Mecp2^{+/y}$ slices, LSP4-2022 decreased the slope of the first fEPSP (Fig. 3, A and B). In contrast, LSP4-2022 treatment did not alter the fEPSP slope in $Mecp2^{-/y}$ slices (Fig. 3, A and B). Furthermore, application of LSP4-2022 significantly increased PPR in $Mecp2^{+/y}$ slices ($P < 0.01$) but had no effect on PPR in $Mecp2^{-/y}$ slices (Fig. 3C).

The loss of LSP4-2022 efficacy in $Mecp2^{-/y}$ brain slices is consistent with an insufficient number of synaptic $mGlu_7$ receptors in the hippocampus to evoke a synaptic depression. To determine whether we could potentiate $mGlu_7$ function, we used two structurally distinct PAMs targeting $mGlu_7$, VU0422288 and VU0155094 (26). This strategy was selected over increasing the concentration of LSP4-2022 to facilitate downstream in vivo experiments, where PAMs can be preferable to agonists for drug development because of their ability to maintain temporal control of receptor activation. VU0422288 and VU0155094 are group III mGlu PAMs that target $mGlu_4$, $mGlu_7$, and $mGlu_8$; however, because of the apparent lack of expression of $mGlu_4$ and $mGlu_8$ at SC-CA1 (31), examining the activity at SC-CA1 should

enhance the detection of an $mGlu_7$ component. We have previously shown that both VU0422288 and VU0155094 potentiate the response to 30 μM LSP4-2022 in slices from wild-type C57/B6 mice (26). We pretreated *Mecp2*$^{-/y}$ slices for 5 min with either 1 μM VU0422288 or 30 μM VU0155094 and then coapplied 1 μM VU0422288 or 30 μM VU0155094 with 30 μM LSP4-2022 for 10 min. Neither VU0422288 nor VU0155094 significantly altered the fEPSP slopes alone, indicating that $mGlu_7$ is not tonically active in *Mecp2*$^{-/y}$ slices under our stimulation conditions (Fig. 3D and fig. S4, A and B). However, when either PAM was coapplied with LSP4-2022, we observed a significant reduction in the fEPSP slope ($P < 0.001$; Fig. 3, D and E, and fig. S4, A to C). Additionally, application of either VU0422288 or VU0155094 with LSP4-2022 significantly increased PPR ($P < 0.001$; Fig. 3, F and G, and fig. S4D). Together, these data indicate that $mGlu_7$ function is reduced in *Mecp2*$^{-/y}$ slices, consistent with the decrease in receptor expression; however, $mGlu_7$ signaling can be restored with a PAM.

Potentiation of $mGlu_7$ rescues LTP deficits and improves hippocampal learning and memory

Deficits in LTP at SC-CA1 synapses have been observed in several mouse models of RTT (20–22). In slices from wild-type C57/B6 mice, we previously found that a high-frequency stimulation (HFS) paradigm induces robust LTP, which can be potentiated by $mGlu_7$ activation (23). In our current experiments, LTP induced by the same HFS was significantly reduced in hippocampal slices from symptomatic *Mecp2*$^{-/y}$ mice ($P < 0.01$; fig. S5A). Decreased $mGlu_7$ expression, coupled with our previous report showing that $mGlu_7$ activation is required for LTP at SC-CA1 synapses (23), led us to hypothesize that attenuated LTP in *Mecp2*$^{-/y}$ slices could be a result of diminished $mGlu_7$ activity. Therefore, we next determined whether potentiation of $mGlu_7$ could rescue LTP. We found that pretreatment of *Mecp2*$^{-/y}$ slices with 1 μM of the group III mGlu receptor PAM VU0422288 resulted in a complete restoration of the LTP response (fig. S5B). We further examined the effects of VU0422288 using a threshold-HFS protocol in *Mecp2*$^{+/y}$ slices and found that VU0422288 administration potentiated LTP, suggesting that the observed effects are not genotype-specific (fig. S5, C and D). Together, these data indicate that potentiation of $mGlu_7$ is sufficient to rescue LTP at SC-CA1 synapses in *Mecp2*$^{-/y}$ mice. Additionally, the finding that application of VU0422288 alone increased fEPSPs after HFS, but not after single pulses (Fig. 3D), indicates that HFS results in sufficient glutamatergic tone at the synapse for a PAM to potentiate $mGlu_7$ function without the need for application of an exogenous agonist.

We next sought to determine whether VU0422288's effects on LTP translated into improvements in learning and memory. Because the most disease-relevant model of RTT is female *Mecp2*$^{+/-}$ mice (32), we first assessed whether $mGlu_7$ expression was decreased in these animals. Similar to what was observed in *Mecp2*$^{-/y}$ mice, we detected a significant decrease in $mGlu_7$ expression in synaptosome preparations from the hippocampus ($P < 0.05$) but not the cortex (Fig. 4A). We next confirmed an absence of LTP at SC-CA1 in brain slices from 20-week-old *Mecp2*$^{+/-}$ mice (Fig. 4B), as has previously been reported (33). We found that bath application of VU0422288 could restore LTP at SC-CA1 in this model as well (Fig. 4B). These results provided the rationale to progress to behavioral experiments in *Mecp2*$^{+/-}$ mice.

The contextual fear conditioning assay is a behavioral task of learning and memory that relies on proper hippocampal function (34) and has been shown to be attenuated in RTT model mice (21, 35). To assess whether $mGlu_7$ potentiation could improve performance in this task, 18- to 20-week-old female *Mecp2*$^{+/-}$ mice were given an intraperitoneal injection of vehicle, $mGlu_{4,7,8}$ PAM VU0422288 (30 mg/kg), or ADX88178 (15 mg/kg) (36) 30 min before training. ADX88178 was chosen as a control for these studies because it is a highly active $mGlu_4$ PAM that also potentiates $mGlu_8$ activity, but not $mGlu_7$ activity, and has been used in both rats and mice for behavioral studies (fig. S6) (36, 37). Using a 10 mg/kg intraperitoneal dose of VU0422288, we measured a total brain concentration of 10.5 μM 1 hour post dose (table S2). The predicted fraction of unbound drug (F_u) for VU0422288 was determined using protein binding assays and was 0.003 in plasma and 0.004 in brain homogenates (that is, 0.3 to 0.4% unbound). The compound exhibited a plasma/brain partitioning coefficient of 1.67 (table S2), resulting in a predicted unbound brain concentration of about 40 nM. Because the in vitro EC_{50} for VU0422288 is 100 nM (26), we increased the dose to 30 mg/kg to achieve sufficient predicted brain exposure to the compound.

Mice were trained in an operant chamber using two mild foot shocks, and associative learning was quantified as the time spent freezing in the same chamber 24 hours after training. Similar to previous reports, we observed significantly less freezing in vehicle-treated *Mecp2*$^{+/-}$ mice compared to *Mecp2*$^{+/+}$ ($P < 0.001$; Fig. 4C) (21, 35). Pre-treatment with VU0422288 (30 mg/kg) had no effect in *Mecp2*$^{+/+}$ animals but resulted in a significant rescue of freezing behavior in *Mecp2*$^{+/-}$ mice ($P < 0.01$; Fig. 4C). Pretreatment with ADX88178 (15 mg/kg) had no effect on contextual fear memory in *Mecp2*$^{+/-}$ mice, suggesting that the observed effects are $mGlu_7$-mediated (Fig. 4C). Nociception in *Mecp2*$^{+/-}$ mice was comparable to *Mecp2*$^{+/+}$ controls, regardless of treatment (fig. S7, A and B).

To assess the effects of $mGlu_7$ potentiation in a cognitive assay not dependent on fear-based memory, we used novel object recognition (NOR). Consistent with previous reports (38), *Mecp2*$^{+/-}$ mice treated with vehicle 30 min before training failed to distinguish between the novel and familiar objects 1 hour after exposure (Fig. 4D). VU0422288 increased the discrimination index in *Mecp2*$^{+/-}$ mice to *Mecp2*$^{+/+}$ control levels. ADX88178 did not provide the same benefit, again indicating that the effect of VU0422288 are likely $mGlu_7$-mediated (Fig. 4D). Because anxiety can affect both conditioned fear and NOR performance, we also conducted an elevated plus maze (EPM) assay, where increased or decreased time in the open arms is indicative of anxiolytic or anxiogenic phenotypes, respectively. Vehicle-treated *Mecp2*$^{+/-}$ mice spent significantly more time than *Mecp2*$^{+/+}$ control mice in the open arms of the EPM ($P < 0.01$), and this phenotype was also significantly reversed by VU0422288 ($P < 0.05$; Fig. 4E). Significant rescue was not observed in ADX88178-treated *Mecp2*$^{+/-}$ mice relative to vehicle-treated *Mecp2*$^{+/-}$ mice; however, the significant impairment relative to vehicle-treated *Mecp2*$^{+/+}$ mice was lost, likely due to the known effects of $mGlu_4$ and $mGlu_8$ on anxiety (39).

To assess social memory and preference, we performed a three-chamber discrimination assay. In this assay, a mouse is placed in a three-chamber testing box and exposed to a stranger mouse (stranger 1). Three hours later, the mouse is returned to the same chamber

and assessed for recognition of stranger 1 relative to a novel mouse (stranger 2). Using the aforementioned compound dosing strategy, *Mecp2*$^{+/+}$ control mice demonstrated recognition and preference for the stranger 2 mouse with vehicle, VU0422288, and ADX88178 treatment (Fig. 4F). Conversely, vehicle- and ADX88178-treated *Mecp2*$^{+/-}$ mice did not distinguish between stranger 1 and stranger 2, indicative of impairments in social recognition and/or preference (Fig. 4F). In contrast, social recognition was normalized in *Mecp2*$^{+/-}$ mice treated with VU0422288, which demonstrated recognition and preference comparable to *Mecp2*$^{+/+}$ controls (Fig. 4F). We further confirmed the role of $mGlu_7$ in both the conditioned fear and social recognition assays by coadministering the group III mGlu PAM VU0422288 with the selective $mGlu_7$ NAM, ADX71743 (29). In these experiments, the benefits of the VU0422288 administration were lost with cotreatment, and $mGlu_7$ NAM–alone treatment disrupted social preference in *Mecp2*$^{+/+}$ mice (fig. S8, A to E). These data, coupled with the experiments described above, demonstrate that potentiation of $mGlu_7$ is sufficient to improve impairments in social, cognitive, and anxiety phenotypes in a mouse model of RTT.

The efficacy of VU0422288 is conserved in repeat dosing paradigms

RTT is a lifelong condition, and thus, it is important that pharmacological interventions maintain efficacy along a protracted timeline. To determine whether tolerance would develop with repeat $mGlu_7$ PAM treatment, we administered VU0422288 (30 mg/kg) or vehicle intraperitoneally daily for 17 days in *Mecp2*$^{+/+}$ and *Mecp2*$^{+/-}$ mice. We then conducted EPM, three-chamber social discrimination, and conditioned fear assays at progressive points throughout the dosing paradigm and measured pharmacokinetic properties after the final dose (fig. S9A). Lethality was not observed with any treatment, and both vehicle- and VU0422288-treated *Mecp2*$^{+/-}$ mice weighed significantly more than *Mecp2*$^{+/+}$ controls ($P < 0.01$ at all time points; fig. S9B). After compound administration on day 17, the pharmacokinetic profile of VU0422288 was comparable between *Mecp2*$^{+/+}$ and *Mecp2*$^{+/-}$ mice, with controls reaching a slightly higher C_{max} in the brain (1445 versus 923 ng/g) (fig. S9C). We observed a significant improvement in RTT-like phenotypes in the contextual fear ($P < 0.05$), EPM ($P < 0.05$), and three-chamber social preference ($P < 0.01$) assays in *Mecp2*$^{+/-}$ mice relative to *Mecp2*$^{+/+}$ mice (fig. S9, D to F), suggesting that tolerance did not occur in these studies. Additionally, we detected a loss of social recognition in *Mecp2*$^{+/+}$ mice treated subchronically with VU0422288, possibly indicating that $mGlu_7$ potentiation has negative consequences on this phenotype in contexts where $mGlu_7$ expression and/or function is normal.

Potentiation of $mGlu_7$ corrects apneas in *Mecp2*$^{+/-}$ mice

One primary RTT phenotype that could have translational value as an outcome measure is the presence of both central and obstructive apneas (40–42), which occur in 65 to 93% of all RTT patients and are readily quantifiable in *Mecp2*$^{+/-}$ mice by whole-body plethysmography (WBP). Several studies implicate hyperexcitation of various brainstem nuclei in mediating central apneas (42–45), and, in rodents, $mGlu_7$ is expressed in the pons and mesencephalon (46). Given that $mGlu_7$ activation would be predicted to temper glutamatergic tone, we next sought to determine whether $mGlu_7$ potentiation altered this core RTT phenotype. Using the treatment groups described above, we performed WBP to

quantify frequency (f), time of inspiration (T_i) and expiration (T_e), and apneas over 30 min of motion-free recording in 20- to 22-week-old *Mecp2*$^{+/-}$ and *Mecp2*$^{+/+}$ mice. Irrespective of genotype, both VU0422288 and ADX88178 administration significantly ($P < 0.05$) decreased breathing rate and increased T_i and T_e (Fig. 5, A to C). Because ADX88178 does not potentiate $mGlu_7$, these data suggest that this effect is likely mediated by $mGlu_4$ and/or $mGlu_8$. For all treatment groups, we observed no differences between *Mecp2*$^{+/+}$ and *Mecp2*$^{+/-}$ mice in f, T_e, or T_i (Fig. 5, A to C). We observed a marked increase in apneas in vehicle-treated *Mecp2*$^{+/-}$ mice, which was significantly decreased by a single dose of VU0422288 to a level that was indistinguishable from *Mecp2*$^{+/+}$ controls ($P < 0.05$; Fig. 5, D to F). This benefit was not observed in ADX88178-treated *Mecp2*$^{+/-}$ mice, again indicating that the effects are $mGlu_7$-mediated (Fig. 5, D to F). Although further work is required to determine the mechanisms responsible for apneas in RTT and where $mGlu_7$ lies in the relevant neurocircuitry, these results provide optimism that $mGlu_7$ modulation may be a viable approach to correct respiratory dysrhythmias and cognitive dysfunction in RTT.

DISCUSSION

Since the identification of *MECP2* as the causative gene for RTT, there has been considerable effort to identify targets regulated by MECP2 that are amenable to drug development (1). Unfortunately, large-scale microarray studies have identified very few genes regulated by MECP2 that are potential druggable targets (10, 11). Here, we describe reductions in $mGlu_7$ expression in total cortex and at the synaptic level in the hippocampus of *Mecp2*$^{-/y}$ and *Mecp2*$^{+/-}$ mice. MECP2 reduction was also observed in autopsy samples from the motor cortex of RTT patients. Decreased synaptic expression of $mGlu_7$ in *Mecp2*$^{-/y}$ and *Mecp2*$^{+/-}$ mice translates into a loss of $mGlu_7$ function at SC-CA1 synapses. We found that treatment with two structurally distinct group III mGlu receptor PAMs, VU0422288 and VU0155094, rescued $mGlu_7$-mediated synaptic transmission at SC-CA1 synapses and that VU0422288 administration also rescued learning and memory, social preference, and anxiety phenotypes and reduced apneas in a mouse model of RTT.

Deficits in LTP at SC-CA1 synapses and in behavioral tasks reliant on proper hippocampal function have been well characterized in mouse models of RTT (20–22). We previously identified that activation of $mGlu_7$ is a necessary component of LTP induction at SC-CA1 synapses (23). This mechanism is mediated by activation of $mGlu_7$ expressed presynaptically on GABAergic interneurons (23). It has previously been reported that loss of *Mecp2* from GABAergic interneurons in mice is sufficient to recapitulate many RTT endophenotypes, including deficits in LTP induction at SC-CA1 (4). Together, these findings suggest that the loss of $mGlu_7$ could be one underlying cause of LTP deficits in mouse models of RTT (20–22). We found that potentiation of $mGlu_7$ is able to rescue LTP and improves deficits in hippocampal-dependent contextual fear and social recognition memory assays, indicating that $mGlu_7$ PAMs can be efficacious in vivo.

In addition to the hippocampus, $mGlu_7$ is also expressed in a variety of other brain regions that overlap with the major symptom domains of RTT (16). In rodents, $mGlu_7$ is expressed in brainstem regions implicated in apneas such as the pons and mesencephalon (46), and we show here that potentiation of $mGlu_7$ decreases the presence of apneas in *Mecp2*$^{+/-}$ mice.

Because many intervention strategies that target apneas also have sedative effects (47, 48), the fact that VU0422288 treatment normalizes respiratory phenotypes in the absence of overt sedation in any of our phenotypic assays is a salient finding. When combined with the learning and memory experiments, these studies suggest that modulation of $mGlu_7$ may be a therapeutic strategy for the treatment of several domains of RTT. Furthermore, because the $mGlu_{4,8}$ PAM (ADX88178) decreased respiratory rate relative to vehicle treatment, these results advocate for the development of selective $mGlu_7$ PAMs, which should be free of this adverse effect.

The dichotomy between *GRM7* mRNA and $mGlu_7$ protein expression remains a limitation for these studies that will merit careful consideration in future experiments. Additionally, our experiments in both *Mecp2*$^{-/y}$ and *Mecp2*$^{+/-}$ demonstrate that total hippocampal $mGlu_7$ expression is not affected, whereas the functional synaptic pool of $mGlu_7$ is decreased. This may be indicative of a primary deficit in $mGlu_7$ trafficking within RTT model mice; however, our current studies were limited to quantifying expression, and more studies will be required to determine whether this is the case. An additional limitation to our work is that, because of the absence of a selective $mGlu_7$ PAM, we used an $mGlu_{4,7,8}$ PAM coupled with parallel experiments using an $mGlu_{4,8}$ PAM and/or an $mGlu_7$ NAM to examine the role of $mGlu_7$ in RTT. Although this strategy suggests that $mGlu_7$ potentiation is beneficial in RTT model mice, it does not exclude the possibility that $mGlu_{4,7}$ or $mGlu_{7,8}$ coactivation is required for efficacy. Future work will be required to determine whether $mGlu_7$ potentiation alone is sufficient to explain the results described in this manuscript.

GPCRs such as $mGlu_7$ are considered to be highly druggable targets because their endogenous function is to integrate external signals into intracellular responses upon ligand binding. This is evident by the fact that molecules targeting GPCRs represent 27% of all U.S. Food and Drug Administration–approved drugs (49). Here, we describe how the loss of MECP2 results in decreased $mGlu_7$ signaling and demonstrate that potentiation of $mGlu_7$ function is sufficient to rescue synaptic plasticity deficits and improve multiple RTT-like phenotypes in mice. These data corroborate other studies suggesting that the pathophysiology of RTT is reversible in mouse models (12, 13, 33, 50). Finally, we have shown that $mGlu_7$ expression is sensitive to pathogenic mutations in *MECP2*, and given that the full range of *MECP2*-related disorders has only recently been appreciated, it is possible that $mGlu_7$ modulators will have broad utility that extends beyond RTT and into other disorders wherein MECP2 expression and function are compromised, such as *MECP2* duplication syndrome and *CDKL5* disorder (51, 52).

MATERIALS AND METHODS

Study design

On the basis of the localization and known function of $mGlu_7$, we hypothesized that disruptions in $mGlu_7$ signaling were contributing to RTT phenotypes, and our research objectives were to both establish its role at the basic science level and determine whether $mGlu_7$ PAMs could positively modify the disease in rodents. The selection of mouse model, sex, and sample size was based on the standards established by the National Institute of Mental Health and RTT research community (32). For phenotypic assays, mice were

assigned randomly to dosing groups, and the quantitation was performed either by a researcher that was blinded to genotype and treatment group or by automated software.

Reporter gene construction and luciferase assay

One thousand base pairs of the *GRM7* promoter was cloned into the pGL4 expression vector (Promega), and *MECP2* was cloned into the pIRESpuro3 vector (Clontech). *MECP2* was transfected into HEK293 cells using FuGENE 6, and luciferase activity was quantified at 48 hours (Promega). The luciferase and *Renilla* luminescence was measured using a Synergy 2 luminescence plate reader (BioTek). The ratio of luciferase luminescence to *Renilla* luminescence was calculated and normalized to the control condition with no *MECP2* transfection and measured in RLU.

Drugs

VU0422288, VU0155094, LSP4-2022, ADX88178, and ADX71743 were synthesized at the Vanderbilt Center for Neuroscience Drug Discovery as described in (23, 26, 30). The potency of ADX88178 at $mGlu_4$, $mGlu_7$, and $mGlu_8$ receptors was determined as described in (26).

Quantitative real-time polymerase chain reaction

Total RNA was prepared from *Mecp2*$^{tm1.1bird}$ (*Mecp2*$^{-/y}$) and *Mecp2*$^{+/y}$ mice and the motor cortex of human samples as described in (12). The Life Technologies gene expression assays used were *Grm4* (Mm01306128_m1), *Grm7* (Mm0118924_m1), and *Gad2* (Mm00484623_m1). Cycle threshold (C_t) values for each sample were normalized to *Gapdh* (Mm03302249_g1) expression, analyzed using the $\Delta\Delta C_t$ method.

Total and synaptosomal protein preparation

For mouse total protein preparation, the cortex, hippocampus, and stri-atum were microdissected from P39 to P55 *Mecp2*$^{-/y}$, 20-week *Mecp2*$^{+/-}$, and control mice. For human motor cortex protein preparation, frozen sections were obtained from the University of Maryland Brain and Tissue Bank, which is a Brain and Tissue Repository of the National Institutes of Health NeuroBioBank, and the Harvard Brain Tissue Resource Center, which is supported in part by Public Health Service contract HHSN-271-2013-00030C. Total protein was prepared as described in (12), and synaptosome preparations were prepared as described in (53).

SDS–polyacrylamide gel electrophoresis and fluorescent Western blotting

Mouse (50 μg) and human (96 μg) proteins were electrophoretically separated using a 7% SDS polyacrylamide gel and then transferred onto a nitrocellulose membrane (Bio-Rad). Membranes were blocked in Odyssey blocking buffer (LI-COR) and probed with anti-$mGlu_7$ (1:1000; Upstate), anti-vGlut2 (1:1000; Abcam), or anti-tubulin primary antibody (1:2500; Abcam). The fluorescent secondary antibodies used were goat anti-rabbit (800 nm) (1:5000; LI-COR) and goat anti-mouse (680 nm) (1:5000; LI-COR). Fluorescence was then quantified using the LI-COR Odyssey imaging system. Values were normalized to tubulin and compared relative to controls.

Extracellular field potential recordings

Coronal brain slices were prepared from P45 to P50 *Mecp2*$^{-/y}$ and 20-week-old *Mecp2*$^{+/-}$ mice as described in (20). During recordings, slices were continuously perfused with artificial cerebrospinal fluid (Fisher) at 32°C. A concentric bipolar stimulating electrode was positioned near the CA3-CA1 border and paired-pulse fEPSPs were recorded in the stratum radiatum of CA1 (0.05 Hz, 20-ms ISI). For basal synaptic transmission experiments, a stable baseline was recorded for 5 to 10 min before drug application. Dimethyl sulfoxide vehicle, 1 μM VU0422288, or 30 μM VU0155094 was bath-applied for 5 min before the addition of 30 μM LSP4-2022 for 10 min followed by a 15-min washout period.

LTP was induced by applying two trains of 100-Hz stimulation (HFS, 1-s duration, 20-s intertrain interval) after a 15- to 20-min baseline. VU0422288 (1 μM) was applied for 10 min before application of HFS. For all electrophysiological experiments, the slopes of three consecutive sweeps were averaged and normalized to the average slope during the baseline period. Data were digitized using a MultiClamp 700B, Digidata 1322A, and pCLAMP 10 software (Molecular Devices).

In vivo pharmacokinetic analysis

VU0422288 (10 mg/kg) was administered intraperitoneally to adult male Sprague-Dawley rats (Harlan Laboratories). Animals were euthanized at progressive time points and decapitated to obtain blood and brain samples. Liquid chromatography mass spectrometry analysis of plasma and brain VU0422288 concentrations was performed as previously described (26, 30). The brain homogenate binding of VU0422288 was determined in rat brain homogenates via equilibrium dialysis using RED (Rapid Equilibrium Dialysis) plates (Thermo Fisher Scientific).

Compound administration for phenotyping

For all assays, either vehicle (10% Tween 80), VU0422288 (30 mg/kg), ADX88178 (15 mg/kg), a combination of VU0422288 (30 mg/kg) and ADX71743 (60 mg/kg), or ADX71743 (60 mg/kg) was dosed via intra-peritoneal injection (10 ml/kg) to 18- to 22-week-old *Mecp2*$^{+/+}$ and *Mecp2*$^{+/-}$ mice (C57/B6, tm1.1 bird allele). Compounds were dosed 30 min before training (contextual fear, novel object, and social preference) or the assay (nociception, EPM, and WBP), such that learning occurred or behavior was assessed at the T_{max} of each compound.

Contextual fear conditioning assay

Contextual fear conditioning was performed using a 10% vanilla odor cue and two 1-s, 0.7-mA foot shocks spaced 30 s apart that were preceded by a tone. Associative learning was quantified 24 hours later as the percent time spent freezing in the same chamber containing the odor cue but without the tone or shock. A nociception assay was also performed by applying a series of mild foot shocks of increasing intensity 15 s apart and progressing as follows: 0.05, 0.1, 0.2, 0.3, 0.4, 0.5, 0.6, and 0.7 mA. Startle response was visually quantified as either a jump or freezing while exploring.

NOR assay

NOR was conducted as described in (54) using the dosing strategy described above. Briefly, mice were placed inside a chamber with two identical objects and allowed to explore for 10 min. The animals were then returned to their home cage. After 1 hour, the mice were placed in the chamber a final time for 10 min, and one of the two objects was replaced with a novel object. The test was video recorded, and the seconds spent directly sniffing each object was scored by a blinded reviewer. Discrimination index was defined as $(\text{Time}_{\text{novel}} - \text{Time}_{\text{familiar}})/(\text{Time}_{\text{novel}} + \text{Time}_{\text{familiar}})$. Direct sniffing in the NOR assay was defined as an approach wherein the mouse's nose either made contact or came in close proximity to the object. All assays were performed under full light conditions (~400 lux) in 33 cm × 33 cm × 41 cm testing chambers.

Elevated plus maze

For EPM, mice were placed on a T-shaped platform, where two of the arms were closed and two were open. The time spent exploring each arm over a 5-min testing period served as a readout of anxiety behavior. The assay was conducted under full light conditions (~400 lux) in the open arms, and the time spent exploring was quantified by ANY-maze software.

Three-chamber social preference assay

Compound-treated mice were placed in a standard three-chamber apparatus and allowed to habituate for a period of 7 min. The mice were then exposed to a novel juvenile mouse (stranger 1) and a toy rubber duck for 7 min and then returned to their home cage. After 3 hours, the animals were placed back within the three-chamber apparatus, and the time spent in the chamber with stranger 1 or a novel stranger (stranger 2) was quantified for 7 min. Animal tracking was performed using ANY-maze software.

Whole-body plethysmography

Unrestrained *Mecp2*$^{+/-}$ and *Mecp2*$^{+/+}$ mice were placed in a WBP recording chamber (Buxco, two-site system) with a continuous inflow of air (1 liter/min). After a habituation period of 45 min, a baseline recording was established for 30 min. Mice were then removed from the chamber, injected intraperitoneally with compound, and reaccli-mated for 30 min, and respirator measurements were made for an additional 30 min. Analysis was performed using FinePointe Research Suite (version 2.3.1.9). Apneas, defined as pauses spanning twice the average expiratory time of the previous 2 min, were quantified using the FinePointe apnea software patch, followed by manual spot checking of the larger data set. Only points of motion-free recording were analyzed. Periods of movement were removed (i) automatically by the FinePointe apnea software, (ii) manually by identifying points where the Δ-chamber volume exceeded the normal breath range, and (iii) at points where the researcher present during the recording noted activity. All filters were applied while the researchers were blinded to genotype and treatment group.

Statistical analyses

Statistics were carried out using Prism 6.0 (GraphPad) and Excel (Microsoft). Data for all graphs are presented in their respective figure legends. All data shown represent means ±

SEM. Statistical significance between groups was determined using two-tailed unpaired or paired Student's *t* tests and one- or two-way ANOVA, with Bonferroni's or individual Student's *t* test post hoc analysis. Sample size, number of replicates, and statistical test are specified in each figure legend.

Supplementary Material

Refer to Web version on PubMed Central for supplementary material.

Acknowledgments

We acknowledge the donation of samples from RTT patient families, and we thank the University of Maryland Brain and Tissue Bank, the Harvard Brain Tissue Resource Center, and Rettsyndrome.org, for their assistance in obtaining this valuable resource.

Funding: R.G.G. was supported by a postdoctoral fellowship from Rettsyndrome.org, NIH T32 AG000260, and NIH T32-MH065215. R.K.S. was supported by a Weatherstone Predoctoral Fellowship from Autism Speaks and the Howard Hughes Medical Institute Certificate Program in Molecular Medicine through Vanderbilt University. N.M.F. was supported by training grant NIH T32 GM007628-36 and the Vanderbilt Program in Molecular Medicine through Vanderbilt University. A.G.W. was supported by a postdoctoral fellowship through the PhRMA Foundation. We also acknowledge U54 MH084659 (C.W.L.), R01 NS031373 (P.J.C.), a Basic Research grant from Rettsyndrome.org (C.M.N.), a Treatment Grant from Autism Speaks (C.M.N.), and R21 MH102548 (C.M.N.).

REFERENCES AND NOTES

1. Amir RE, Van den Veyver IB, Wan M, Tran CQ, Francke U, Zoghbi HY. Rett syndrome is caused by mutations in X-linked *MECP2*, encoding methyl-CpG-binding protein 2. Nat Genet. 1999; 23:185–188. [PubMed: 10508514]
2. Hagberg B. Clinical manifestations and stages of Rett syndrome. Ment Retard Dev Disabil Res Rev. 2002; 8:61–65. [PubMed: 12112728]
3. Chen RZ, Akbarian S, Tudor M, Jaenisch R. Deficiency of methyl-CpG binding protein-2 in CNS neurons results in a Rett-like phenotype in mice. Nat Genet. 2001; 27:327–331. [PubMed: 11242118]
4. Chao HT, Chen H, Samaco RC, Xue M, Chahrour M, Yoo J, Neul JL, Gong S, Lu HC, Heintz N, Ekker M, Rubenstein JLR, Noebels JL, Rosenmund C, Zoghbi HY. Dysfunction in GABA signalling mediates autism-like stereotypies and Rett syndrome phenotypes. Nature. 2010; 468:263–269. [PubMed: 21068835]
5. Adachi M, Autry AE, Covington HE III, Monteggia LM. MeCP2-mediated transcription repression in the basolateral amygdala may underlie heightened anxiety in a mouse model of Rett syndrome. J Neurosci. 2009; 29:4218–4227. [PubMed: 19339616]
6. Fyffe SL, Neul JL, Samaco RC, Chao HT, Ben-Shachar S, Moretti P, McGill BE, Goulding EH, Sullivan E, Tecott LH, Zoghbi HY. Deletion of *Mecp2* in *Sim1*-expressing neurons reveals a critical role for MeCP2 in feeding behavior, aggression, and the response to stress. Neuron. 2008; 59:947–958. [PubMed: 18817733]
7. Samaco RC, Mandel-Brehm C, Chao HT, Ward CS, Fyffe-Maricich SL, Ren J, Hyland K, Thaller C, Maricich SM, Humphreys P, Greer JJ, Percy A, Glaze DG, Zoghbi HY, Neul JL. Loss of MeCP2 in aminergic neurons causes cell-autonomous defects in neurotransmitter synthesis and specific behavioral abnormalities. Proc Natl Acad Sci USA. 2009; 106:21966–21971. [PubMed: 20007372]
8. Zhang Y, Cao SX, Sun P, He HY, Yang CH, Chen XJ, Shen CJ, Wang XD, Chen Z, Berg DK, Duan S, Li XM. Loss of MeCP2 in cholinergic neurons causes part of RTT-like phenotypes via α7 receptor in hippocampus. Cell Res. 2016; 26:728–742. [PubMed: 27103432]
9. Chahrour M, Jung SY, Shaw C, Zhou X, Wong STC, Qin J, Zoghbi HY. MeCP2, a key contributor to neurological disease, activates and represses transcription. Science. 2008; 320:1224–1229. [PubMed: 18511691]

10. Ben-Shachar S, Chahrour M, Thaller C, Shaw CA, Zoghbi HY. Mouse models of MeCP2 disorders share gene expression changes in the cerebellum and hypothalamus. Hum Mol Genet. 2009; 18:2431–2442. [PubMed: 19369296]
11. Tudor M, Akbarian S, Chen RZ, Jaenisch R. Transcriptional profiling of a mouse model for Rett syndrome reveals subtle transcriptional changes in the brain. Proc Natl Acad Sci USA. 2002; 99:15536–15541. [PubMed: 12432090]
12. Gogliotti RG, Senter RK, Rook JM, Ghoshal A, Zamorano R, Malosh C, Stauffer SR, Bridges TM, Bartolome JM, Daniels JS, Jones CK, Lindsley CW, Conn PJ, Niswender CM. mGlu5 positive allosteric modulation normalizes synaptic plasticity defects and motor phenotypes in a mouse model of Rett syndrome. Hum Mol Genet. 2016; 25:1990–2004. [PubMed: 26936821]
13. Kron M, Lang M, Adams IT, Sceniak M, Longo F, Katz DM. A BDNF loop-domain mimetic acutely reverses spontaneous apneas and respiratory abnormalities during behavioral arousal in a mouse model of Rett syndrome. Dis Model Mech. 2014; 7:1047–1055. [PubMed: 25147297]
14. Jellinger K, Armstrong D, Zoghbi HY, Percy AK. Neuropathology of Rett syndrome. Acta Neuropathol. 1988; 76:142–158. [PubMed: 2900587]
15. Shepherd GMG, Katz DM. Synaptic microcircuit dysfunction in genetic models of neurodevelopmental disorders: Focus on Mecp2 and Met. Curr Opin Neurobiol. 2011; 21:827–833. [PubMed: 21733672]
16. Bradley SR, Rees HD, Yi H, Levey AI, Conn PJ. Distribution and developmental regulation of metabotropic glutamate receptor 7a in rat brain. J Neurochem. 1998; 71:636–645. [PubMed: 9681454]
17. Rush LJ, Raval A, Funchain P, Johnson AJ, Smith L, Lucas DM, Bembea M, Liu TH, Heerema NA, Rassenti L, Liyanarachchi S, Davuluri R, Byrd JC, Plass C. Epigenetic profiling in chronic lymphocytic leukemia reveals novel methylation targets. Cancer Res. 2004; 64:2424–2433. [PubMed: 15059895]
18. Dalezios Y, Luján R, Shigemoto R, Roberts JDB, Somogyi P. Enrichment of mGluR7a in the presynaptic active zones of GABAergic and non-GABAergic terminals on interneurons in the rat somatosensory cortex. Cereb Cortex. 2002; 12:961–974. [PubMed: 12183395]
19. Somogyi P, Dalezios Y, Luján R, Roberts JDB, Watanabe M, Shigemoto R. High level of mGluR7 in the presynaptic active zones of select populations of GABAergic terminals innervating interneurons in the rat hippocampus. Eur J Neurosci. 2003; 17:2503–2520. [PubMed: 12823458]
20. Asaka Y, Jugloff DGM, Zhang L, Eubanks JH, Fitzsimonds RM. Hippocampal synaptic plasticity is impaired in the *Mecp2*-null mouse model of Rett syndrome. Neurobiol Dis. 2006; 21:217–227. [PubMed: 16087343]
21. Moretti P, Levenson JM, Battaglia F, Atkinson R, Teague R, Antalffy B, Armstrong D, Arancio O, Sweatt JD, Zoghbi HY. Learning and memory and synaptic plasticity are impaired in a mouse model of Rett syndrome. J Neurosci. 2006; 26:319–327. [PubMed: 16399702]
22. Weng SM, McLeod F, Bailey MES, Cobb SR. Synaptic plasticity deficits in an experimental model of Rett syndrome: Long-term potentiation saturation and its pharmacological reversal. Neuroscience. 2011; 180:314–321. [PubMed: 21296130]
23. Klar R, Walker AG, Ghose D, Grueter BA, Engers DW, Hopkins CR, Lindsley CW, Xiang Z, Conn PJ, Niswender CM. Activation of metabotropic glutamate receptor 7 is required for induction of long-term potentiation at SC-CA1 synapses in the hippocampus. J Neurosci. 2015; 35:7600–7615. [PubMed: 25972184]
24. Callaerts-Vegh Z, Beckers T, Ball SM, Baeyens F, Callaerts PF, Cryan JF, Molnar E, D'Hooge R. Concomitant deficits in working memory and fear extinction are functionally dissociated from reduced anxiety in metabotropic glutamate receptor 7-deficient mice. J Neurosci. 2006; 26:6573–6582. [PubMed: 16775145]
25. Hölscher C, Schmid S, Pilz PKD, Sansig G, van der Putten H, Plappert CF. Lack of the metabotropic glutamate receptor subtype 7 selectively impairs short-term working memory but not long-term memory. Behav Brain Res. 2004; 154:473–481. [PubMed: 15313036]
26. Jalan-Sakrikar N, Field JR, Klar R, Mattmann ME, Gregory KJ, Zamorano R, Engers DW, Bollinger SR, Weaver CD, Days EL, Lewis LM, Utley TJ, Hurtado M, Rigault D, Acher F, Walker AG, Melancon BJ, Wood MR, Lindsley CW, Conn PJ, Xiang Z, Hopkins CR, Niswender CM.

Identification of positive allosteric modulators VU0155094 (ML397) and VU0422288 (ML396) reveals new insights into the biology of metabotropic glutamate receptor 7. ACS Chem Neurosci. 2014; 5:1221–1237. [PubMed: 25225882]

27. Guy J, Hendrich B, Holmes M, Martin JE, Bird A. A mouse *Mecp2*-null mutation causes neurological symptoms that mimic Rett syndrome. Nat Genet. 2001; 27:322–326. [PubMed: 11242117]
28. Bedogni F, Cobolli Gigli C, Pozzi D, Rossi RL, Scaramuzza L, Rossetti G, Pagani M, Kilstrup-Nielsen C, Matteoli M, Landsberger N. Defects during *Mecp2* null embryonic cortex development precede the onset of overt neurological symptoms. Cereb Cortex. 2016; 26:2517–2529. [PubMed: 25979088]
29. Kalinichev M, Rouillier M, Girard F, Royer-Urios I, Bournique B, Finn T, Charvin D, Campo B, Le Poul E, Mutel V, Poli S, Neale SA, Salt TE, Lütjens R. ADX71743, a potent and selective negative allosteric modulator of metabotropic glutamate receptor 7: In vitro and in vivo characterization. J Pharmacol Exp Ther. 2013; 344:624–636. [PubMed: 23257312]
30. Goudet C, Vilar B, Courtiol T, Deltheil T, Bessiron T, Brabet I, Oueslati N, Rigault D, Bertrand HO, McLean H, Daniel H, Amalric M, Acher F, Pin JP. A novel selective metabotropic glutamate receptor 4 agonist reveals new possibilities for developing subtype selective ligands with therapeutic potential. FASEB J. 2012; 26:1682–1693. [PubMed: 22223752]
31. Ayala JE, Niswender CM, Luo Q, Banko JL, Conn PJ. Group III mGluR regulation of synaptic transmission at the SC-CA1 synapse is developmentally regulated. Neuropharmacology. 2008; 54:804–814. [PubMed: 18255102]
32. Katz DM, Berger-Sweeney JE, Eubanks JH, Justice MJ, Neul JL, Pozzo-Miller L, Blue ME, Christian D, Crawley JN, Giustetto M, Guy J, Howell CJ, Kron M, Nelson SB, Samaco RC, Schaevitz LR, St Hillaire-Clarke C, Young JL, Zoghbi HY, Mamounas LA. Preclinical research in Rett syndrome: Setting the foundation for translational success. Dis Model Mech. 2012; 5:733–745. [PubMed: 23115203]
33. Guy J, Gan J, Selfridge J, Cobb S, Bird A. Reversal of neurological defects in a mouse model of Rett syndrome. Science. 2007; 315:1143–1147. [PubMed: 17289941]
34. Phillips RG, LeDoux JE. Differential contribution of amygdala and hippocampus to cued and contextual fear conditioning. Behav Neurosci. 1992; 106:274–285. [PubMed: 1590953]
35. Pelka GJ, Watson CM, Radziewic T, Hayward M, Lahooti H, Christodoulou J, Tam PPL. *Mecp2* deficiency is associated with learning and cognitive deficits and altered gene activity in the hippocampal region of mice. Brain. 2006; 129:887–898. [PubMed: 16467389]
36. Le Poul E, Boléa C, Girard F, Poli S, Charvin D, Campo B, Bortoli J, Bessif A, Luo B, Koser AJ, Hodge LM, Smith KM, DiLella AG, Liverton N, Hess F, Browne SE, Reynolds IJ. A potent and selective metabotropic glutamate receptor 4 positive allosteric modulator improves movement in rodent models of Parkinson's disease. J Pharmacol Exp Ther. 2012; 343:167–177. [PubMed: 22787118]
37. Kalinichev M, Le Poul E, Bolea C, Girard F, Campo B, Fonsi M, Royer-Urios I, Browne SE, Uslaner JM, Davis MJ, Raber J, Duvoisin R, Bate ST, Reynolds IJ, Poli S, Celanire S. Characterization of the novel positive allosteric modulator of the metabotropic glutamate receptor 4 ADX88178 in rodent models of neuropsychiatric disorders. J Pharmacol Exp Ther. 2014; 350:495–505. [PubMed: 24947466]
38. Garg SK, Lioy DT, Cheval H, McGann JC, Bissonnette JM, Murtha MJ, Foust KD, Kaspar BK, Bird A, Mandel G. Systemic delivery of MeCP2 rescues behavioral and cellular deficits in female mouse models of Rett syndrome. J Neurosci. 2013; 33:13612–13620. [PubMed: 23966684]
39. Davis MJ, Duvoisin RM, Raber J. Related functions of mGlu4 and mGlu8. Pharmacol Biochem Behav. 2013; 111:11–16. [PubMed: 23948069]
40. Weese-Mayer DE, Lieske SP, Boothby CM, Kenny AS, Bennett HL, Silvestri JM, Ramirez JM. Autonomic nervous system dysregulation: Breathing and heart rate perturbation during wakefulness in young girls with Rett syndrome. Pediatr Res. 2006; 60:443–449. [PubMed: 16940240]
41. Kerr AM. A review of the respiratory disorder in the Rett syndrome. Brain Dev. 1992; 14:S43–S45. [PubMed: 1626633]

42. Katz DM, Dutschmann M, Ramirez JM, Hilaire G. Breathing disorders in Rett syndrome: Progressive neurochemical dysfunction in the respiratory network after birth. Respir Physiol Neurobiol. 2009; 168:101–108. [PubMed: 19394452]
43. Stettner GM, Huppke P, Brendel C, Richter DW, Gärtner J, Dutschmann M. Breathing dysfunctions associated with impaired control of postinspiratory activity in *Mecp2*$^{-/y}$ knockout mice. J Physiol. 2007; 579:863–876. [PubMed: 17204503]
44. Kron M, Zimmermann JL, Dutschmann M, Funke F, Müller M. Altered responses of MeCP2-deficient mouse brain stem to severe hypoxia. J Neurophysiol. 2011; 105:3067–3079. [PubMed: 21471397]
45. Kron M, Howell CJ, Adams IT, Ransbottom M, Christian D, Ogier M, Katz DM. Brain activity mapping in *Mecp2* mutant mice reveals functional deficits in forebrain circuits, including key nodes in the default mode network, that are reversed with ketamine treatment. J Neurosci. 2012; 32:13860–13872. [PubMed: 23035095]
46. Lourenço Neto F, Schadrack J, Platzer S, Zieglgänsberger W, Tölle TR, Castro-Lopes JM. Expression of metabotropic glutamate receptors mRNA in the thalamus and brainstem of monoarthritic rats. Brain Res Mol Brain Res. 2000; 81:140–154. [PubMed: 11000486]
47. Viemari JC, Roux JC, Tryba AK, Saywell V, Burnet H, Peña F, Zanella S, Bévengut M, Barthelemy-Requin M, Herzing LBK, Moncla A, Mancini J, Ramirez JM, Villard L, Hilaire G. Mecp2 deficiency disrupts norepinephrine and respiratory systems in mice. J Neurosci. 2005; 25:11521–11530. [PubMed: 16354910]
48. Ren J, Ding X, Funk GD, Greer JJ. Anxiety-related mechanisms of respiratory dysfunction in a mouse model of Rett syndrome. J Neurosci. 2012; 32:17230–17240. [PubMed: 23197715]
49. Overington JP, Al-Lazikani B, Hopkins AL. How many drug targets are there? Nat Rev Drug Discov. 2006; 5:993–996. [PubMed: 17139284]
50. Castro J, Garcia RI, Kwok S, Banerjee A, Petravicz J, Woodson J, Mellios N, Tropea D, Sur M. Functional recovery with recombinant human IGF1 treatment in a mouse model of Rett Syndrome. Proc Natl Acad Sci USA. 2014; 111:9941–9946. [PubMed: 24958891]
51. Mari F, Azimonti S, Bertani I, Bolognese F, Colombo E, Caselli R, Scala E, Longo I, Grosso S, Pescucci C, Ariani F, Hayek G, Balestri P, Bergo A, Badaracco G, Zappella M, Broccoli V, Renieri A, Kilstrup-Nielsen C, Landsberger N. CDKL5 belongs to the same molecular pathway of MeCP2 and it is responsible for the early-onset seizure variant of Rett syndrome. Hum Mol Genet. 2005; 14:1935–1946. [PubMed: 15917271]
52. Collins AL, Levenson JM, Vilaythong AP, Richman R, Armstrong DL, Noebels JL, David Sweatt J, Zoghbi HY. Mild overexpression of MeCP2 causes a progressive neurological disorder in mice. Hum Mol Genet. 2004; 13:2679–2689. [PubMed: 15351775]
53. Fentress HM, Klar R, Krueger JJ, Sabb T, Redmon SN, Wallace NM, Shirey-Rice JK, Hahn MK. Norepinephrine transporter heterozygous knockout mice exhibit altered transport and behavior. Genes Brain Behav. 2013; 12:749–759. [PubMed: 24102798]
54. Leger M, Quiedeville A, Bouet V, Haelewyn B, Boulouard M, Schumann-Bard P, Freret T. Object recognition test in mice. Nat Protoc. 2013; 8:2531–2537. [PubMed: 24263092]

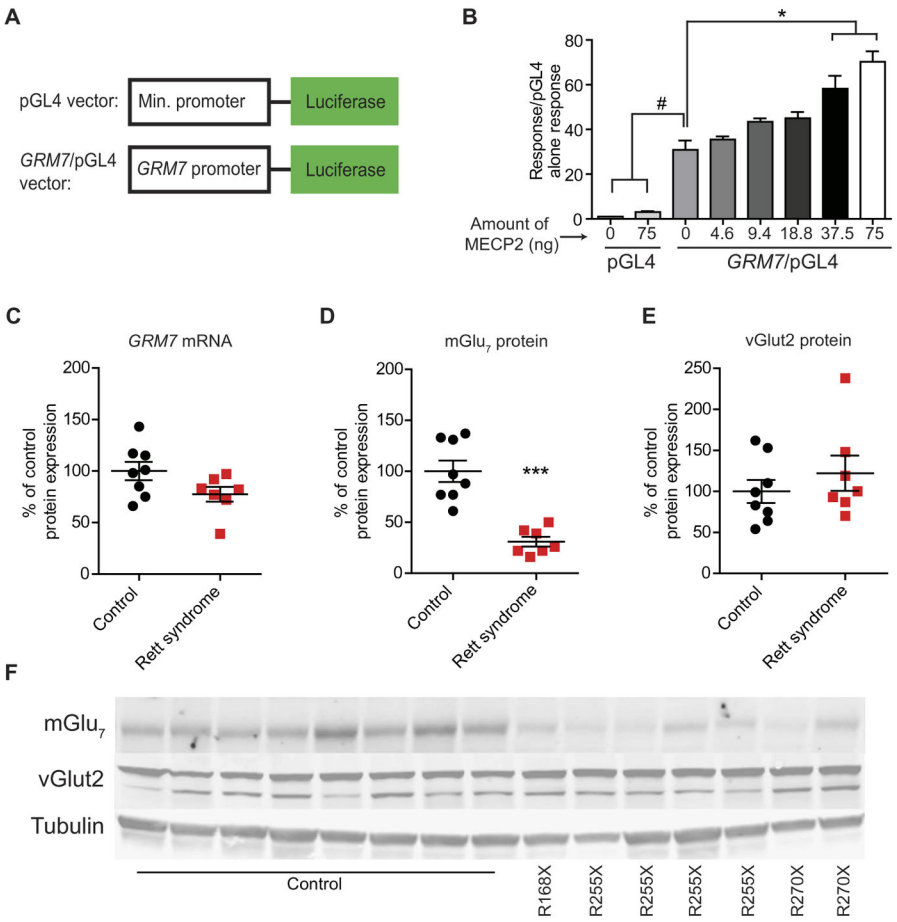

Fig. 1. $mGlu_7$ expression is reduced in RTT autopsy samples

(**A**) Diagram of luciferase reporter constructs. (**B**) Bar graph showing the effect of transfection of increasing amounts of human *MECP2* plasmid on luciferase expression from the pGL4 vector with and without the *GRM7* promoter [$^{\#}P < 0.0001$ and $*P < 0.0001$, one-way analysis of variance (ANOVA) with Bonferroni's post hoc; $n = 3$]. (**C**) *GRM7* messenger RNA (mRNA) expression in the motor cortex of control and RTT autopsy samples ($P = 0.07$, two-tailed Student's t test; $n = 7$ to 8 biological replicates, df = 13). (**D**) $mGlu_7$ ($^{***}P < 0.0001$, two-tailed Student's t test; $n = 7$ to 8, df = 13) and (**E**) vGlut2 ($P = 0.39$, two-tailed Student's t test; $n = 7$ to 8, df = 13) protein expression in control and RTT autopsy samples. (**F**) Representative Western blots showing $mGlu_7$ and vGlut2 expression in control and RTT motor cortex samples. *MECP2* mutations are listed below the representative images.

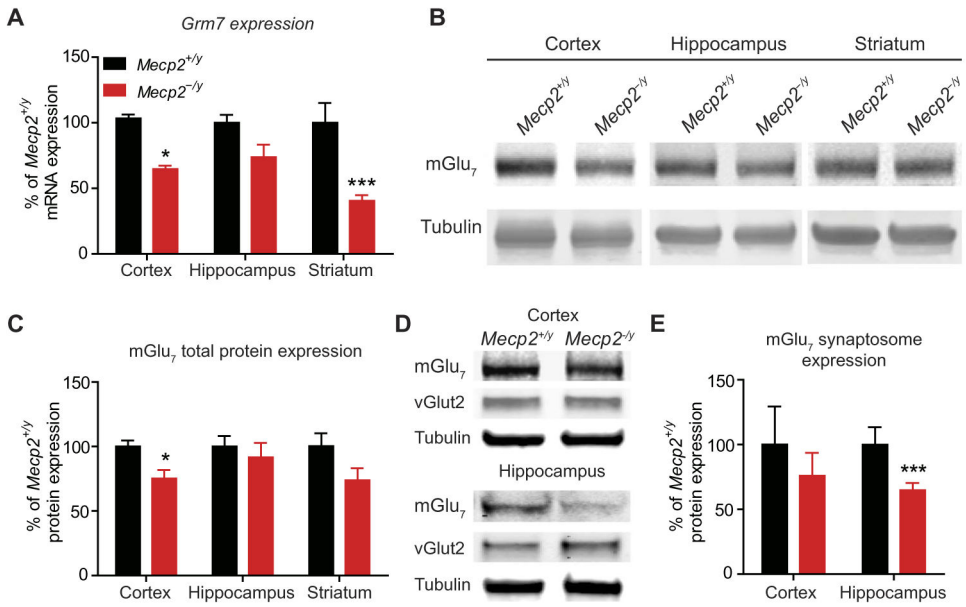

Fig. 2. *Grm7* and mGlu$_7$ expression is decreased in *Mecp2*$^{-/y}$ mice

(**A**) *Grm7* mRNA expression in total cortex (*$P < 0.05$), hippocampus ($P > 0.05$), and striatum (***$P < 0.001$) tissue samples from symptomatic *Mecp2*$^{-/y}$ mice relative to *Mecp2*$^{+/y}$ mice ($P < 0.0001$, two-way ANOVA, genotype × brain region, with Bonferroni's post hoc; $n = 3$ to 5, df = 3, 21). (**B**) Representative Western blots for mGlu$_7$ total protein expression from cortex, hippocampus, and striatum in *Mecp2*$^{+/y}$ and *Mecp2*$^{-/y}$ mice. (**C**) Quantification of mGlu$_7$ total protein expression in the cortex (*$P < 0.05$), hippocampus ($P > 0.05$), and striatum ($P > 0.05$) of *Mecp2*$^{-/y}$ mice (two-way ANOVA, genotype × brain region, with Bonferroni's post hoc; $n = 7$ control and 8 RTT, df = 3, 13). (**D**) Representative synaptosome Western blots for mGlu$_7$ and vGlut2. (**E**) Quantification of mGlu$_7$ expression in synaptosomes prepared from cortex ($P > 0.05$) and hippocampus (***$P < 0.001$) tissue samples from *Mecp2*$^{-/y}$ mice. Two-way ANOVA, genotype × brain region with Bonferroni's post hoc, $P < 0.003$, $n = 5$ samples from individual mice, df = 1, 16.

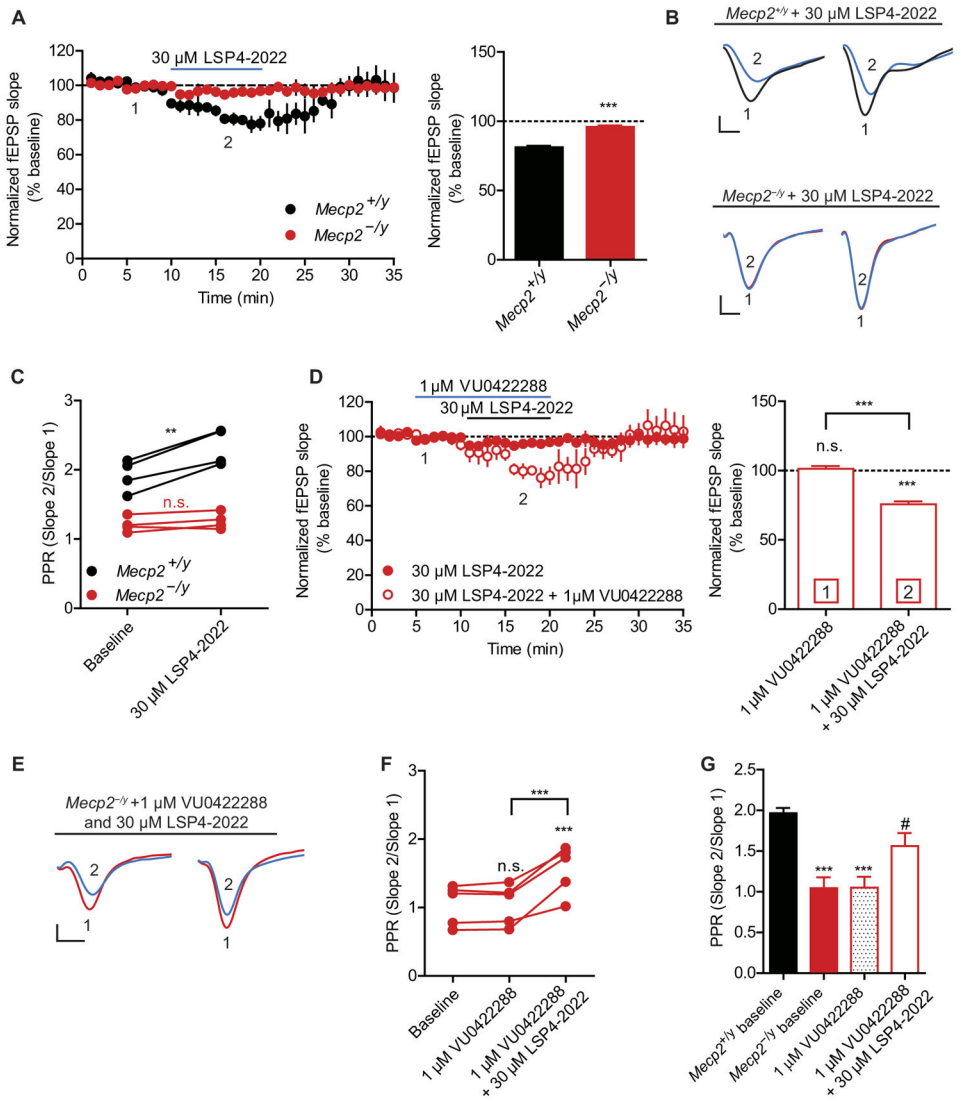

Fig. 3. mGlu $_7$ function is impaired in *Mecp2*$^{-/y}$ slices and can be restored by application of VU0422288

Recordings performed at SC-CA1 synapses. (**A**) Effect of bath application of LSP4-2022 (blue line) on fEPSP slope in *Mecp2*$^{+/y}$ and *Mecp2*$^{-/y}$ slices. *Mecp2*$^{+/y}$ versus *Mecp2*$^{-/y}$ [***$P < 0.0001$, two-tailed Student's t test; $n = 4, 4$ (slices, mice), df = 6]. (**B**) Sample traces of fEPSPs before (1) and during (2) LSP4-2022 treatment in slices from *Mecp2*$^{+/y}$ and *Mecp2*$^{-/y}$ mice. (**C**) PPR after application of LSP4-2022 in *Mecp2*$^{+/y}$ and *Mecp2*$^{-/y}$ slices (**$P = 0.003$, two-tailed paired t test; $n = 4, 4$, df = 3). n.s., not significant. (**D**) Effects of pretreatment with VU0422288 alone and in combination with LSP4-2022 in *Mecp2*$^{-/y}$ slices. *Mecp2*$^{-/y}$ baseline is from (A). ***$P < 0.0001$, one-way repeated-measures ANOVA with Bonferonni's post hoc; $n = 4, 4$, df = 4,8. (**E**) Sample traces of fEPSPs during baseline (1) and after application of VU0422288 and LSP4-2022 (2) in slices from *Mecp2*$^{-/y}$ mice. (**F**) PPR after application of VU0422288 and LSP4-2022 in *Mecp2*$^{-/y}$ slices. $P < 0.0001$, one-way repeated-measures ANOVA with Bonferonni's post hoc; $n = 5, 5$, df = 4, 8. ***$P <$ 0.001 VU0422288 alone versus VU0422288 + LSP4-2022 and ***$P < 0.001$ VU0422288 +

LSP4-2022 versus baseline. (**G**) Post hoc analysis of PPR comparing baseline *Mecp2*$^{+/y}$ levels relative to *Mecp2*$^{-/y}$ baseline (***$P < 0.001$), VU0422288 alone (***$P < 0.001$), and VU0422288 + LSP4-2022 ($^{\#}P < 0.05$ relative to *Mecp2*$^{-/y}$ baseline). Two-tailed Student's *t* test. Scale bars, 0.2 mV by 2 ms (B and E).

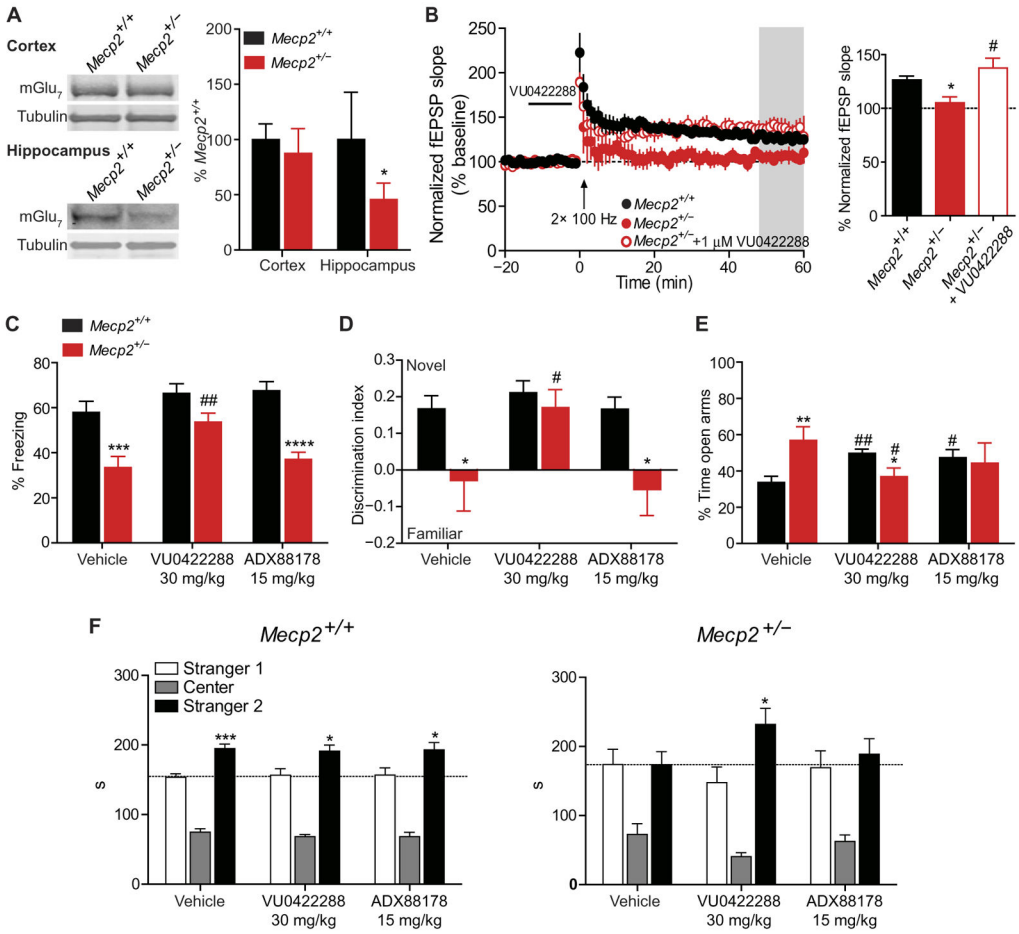

Fig. 4. VU0422288 rescues synaptic plasticity defects and learning and memory phenotypes in *Mecp2*$^{+/-}$ mice

(**A**) $mGlu_7$ expression in synaptosome preparations from the cortex ($P > 0.05$) and hippocampus ($^{*}P < 0.05$) of *Mecp2*$^{+/+}$ and *Mecp2*$^{+/-}$ mice. $n = 7$ per genotype, two-tailed Student's *t* test. (**B**) LTP in *Mecp2*$^{+/+}$ (filled black circles), *Mecp2*$^{+/-}$ ($^{*}P < 0.05$ relative to *Mecp2*$^{+/+}$, filled red circles), and *Mecp2*$^{+/-}$ slices pretreated with VU0422288 ($^{\#}P < 0.05$ relative to *Mecp2*$^{+/-}$ untreated, empty red circles). The gray bar represents the area from which LTP was measured in the accompanying bar graph. One-way ANOVA with Student's *t* test post hoc; $n = 4$ to 5, 4 (slices, mice). (**C**) Contextual fear conditioning in *Mecp2*$^{+/+}$ and *Mecp2*$^{+/-}$ mice treated with vehicle ($n = 22$ and 16), VU0422288 ($n = 17$ and 15), and ADX88178 ($n = 10$ and 15). $^{***}P < 0.001$, $^{\#\#}P < 0.01$, $^{****}P < 0.0001$, two-way ANOVA with Student's *t* test post hoc analysis; df = 2, 89. # denotes within-genotype comparison. (**D**) NOR in *Mecp2*$^{+/+}$ and *Mecp2*$^{+/-}$ mice treated with vehicle, VU0422288 and ADX88178. $^{*}P < 0.05$, $^{\#}P < 0.05$, two-tailed Student's *t* test; $n = 10$ per genotype per treatment. (**E**) EPM in *Mecp2*$^{+/+}$ and *Mecp2*$^{+/-}$ mice treated with vehicle, VU0422288, and ADX88178. $^{**}P < 0.01$, $^{*}P < 0.05$, $^{\#\#}P < 0.01$, $^{\#}P < 0.05$, two-tailed Student's *t* test; $n = 10$ per genotype per treatment. * denotes within-treatment comparison, # denotes within-genotype comparison. (**F**) Social preference assay in *Mecp2*$^{+/+}$ and *Mecp2*$^{+/-}$ mice treated

with vehicle, VU0422288, and ADX88178. ***$P < 0.001$, *$P < 0.05$, two-tailed Student's t test, $n = 9$ to 12 per treatment.

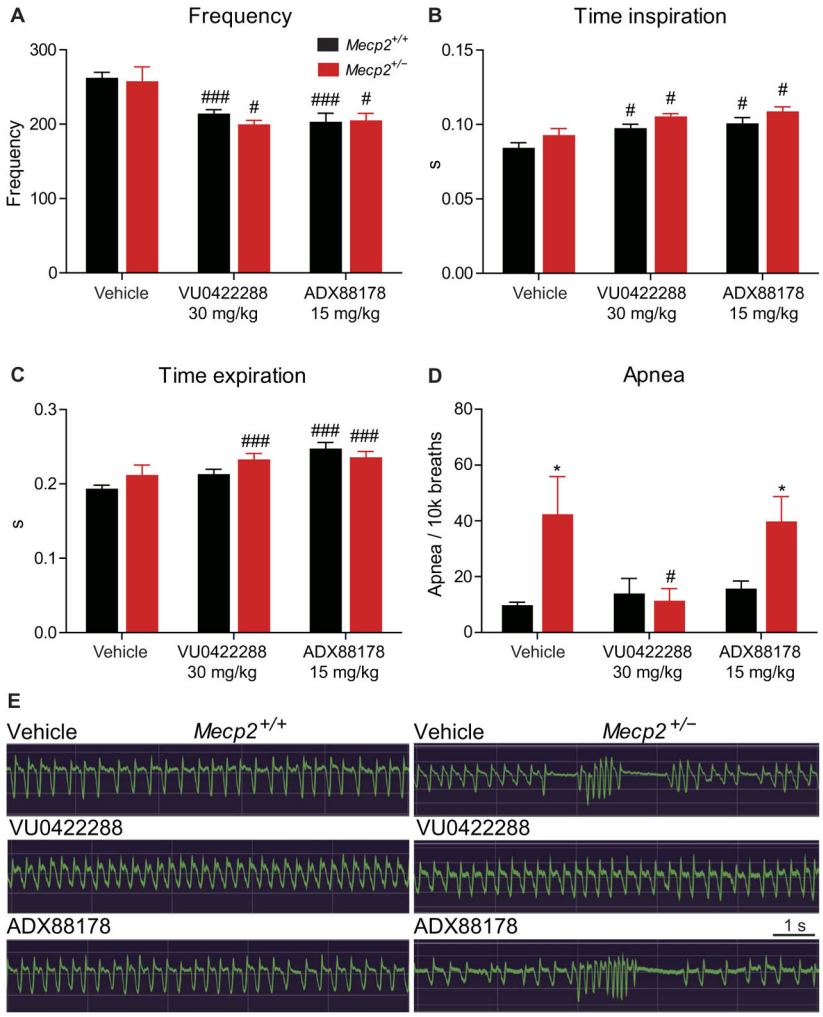

Fig. 5. VU0422288 reduces the number of apneas in *Mecp2*$^{+/-}$ mice. WBP

(**A**) Average breath rate over 30 min in *Mecp2*$^{+/+}$ (black) and *Mecp2*$^{+/-}$ (red) mice in response to vehicle (n = 14 and 11), VU0422288 (n = 11 and 11), and ADX88178 (n = 11 and 14) treatment. $^{\#\#\#}P < 0.001$, $^{\#}P < 0.05$, two-way ANOVA with Student's t test post hoc. # denotes within-genotype comparison. (**B** and **C**) Effects of vehicle, VU0422288, and ADX88178 treatment in *Mecp2*$^{+/+}$ and *Mecp2*$^{+/-}$ mice on (B) inspiration and (C) expiration time. $^{\#\#\#}P < 0.001$, $^{\#}P < 0.05$, two-way ANOVA with Student's t test post hoc. (**D**) Quantification of apneas per 10,000 breaths in *Mecp2*$^{+/+}$ and *Mecp2*$^{+/-}$ treated with vehicle, VU0422288, and ADX88178. $^{*}P < 0.001$, $^{\#}P < 0.05$, two-way ANOVA with Student's t test post hoc. (**E**) Sample plethysmography traces.